

Broadband excitation and collection in fiber-optic nonlinear endomicroscopy

Navin Prakash Ghimire, Hongchun Bao, and Min Gu^{a)}

Centre for Micro-Photonics, Faculty of Engineering & Industrial Sciences, Swinburne University of Technology, Hawthorn, Victoria 3122, Australia

(Received 18 December 2012; accepted 27 July 2013; published online 13 August 2013)

Broadband excitation and collection in a fiber-optic nonlinear endomicroscope are realized by using a single hollow-core double-clad photonic crystal fiber and a gradient index lens. Femtosecond pulses with central wavelengths in the range of 750–850 nm can be directly delivered through the core of the fiber for nonlinear excitation without pre-chirping. A gradient index lens with numerical aperture 0.8 designed to operate over the near-infrared wavelength range is used for focusing the laser beam from the fiber for nonlinear excitation and for collecting the fluorescent signal from the sample. This compact system is suitable to perform nonlinear imaging of multiple fluorophors in the wavelength range of 750–850 nm. © 2013 AIP Publishing LLC. [<http://dx.doi.org/10.1063/1.4818750>]

Nonlinear microscopic imaging is a powerful bio-imaging tool because of its high resolution and high penetration depth compared with other methods of imaging.^{1–3} A fiber based system has advantages of flexibility and compactness for routine use in a clinical environment and *in-vivo* imaging studies. Different fiber types have been employed in nonlinear microscopic imaging systems over a decade to improve the image quality by efficient excitation and collection of the fluorescence signal.^{4–7} A major hurdle with fiber-optic nonlinear microscopic imaging is still imposed by the group velocity dispersion in fibers. Group velocity dispersion increases the temporal pulse width of ultra-fast pulses, severely degrading the excitation efficiency. To solve this optical dispersion problem, a pre-chirp unit external to a fiber is normally used in fiber-optic nonlinear imaging systems for dispersion compensation.^{8–15} A pre-chirp unit generally employs grating pairs, prisms, chirp mirrors, and acoustic-optics modulators (AOM).^{16,17} By adjusting the distance between mirrors/prisms/gratings, the angular orientation of these components, and the beam size, the different frequency components of a pulsed beam obtain different optical path lengths and thus compensate for the chromatic dispersion in the fiber.¹⁸ However, endoscopic systems with a pre-chirp unit are not only cumbersome to operate but also limited for dispersion compensation for pulsed beams with different central wavelengths. For this reason, the design and operation of fiber-optic nonlinear imaging systems is limited to a single near-infrared (NIR) wavelength until recently.

In this paper, we demonstrate the feasibility of broadband excitation and collection in a single fiber based nonlinear endomicroscopy system using a piece of hollow-core photonic crystal fiber (HC-PCF) integrated with a graded index (GRIN) lens. A HC-PCF is unique for the use in nonlinear endoscopic imaging over solid-core silica fibers because of its low chromatic dispersion, low nonlinearity, low loss, and a high damage threshold.^{19,20} A HC-PCF is the most efficient fiber delivery medium among fiber types, as

the optical power in the HC-PCF propagates in the air medium, which results in low transmission losses, low nonlinearity, and low scattering.^{20–23} In addition, this kind of fiber has no Fresnel loss in free space coupling and gives a low background signal level.^{24,25} Single mode propagation at the 800 nm wavelength regime can be achieved in a HC-PCF without sacrificing of the fiber core size. Further, a HC-PCF with zero group velocity dispersion in the visible to NIR wavelength range and having large cladding numerical aperture (NA) with a large cladding diameter allows us to have a high collection efficiency of the fluorescent signal in nonlinear imaging.

Although the delivery of femtosecond pulses through a HC-PCF has been studied for nonlinear excitation, no endoscopy imaging has been achieved by collecting the fluorescent signal through the cladding of the same piece of the fiber.^{7,26–31} Even for the investigation into a microscopy imaging system, the same piece of the HC-PCF has not been used both for broadband nonlinear excitation and broadband fluorescent signal collection. The collection of the fluorescent signal in these systems is still conducted using a separate narrow band fiber other than the HC-PCF.^{7,26–31} A single fiber endomicroscopy system using a double-clad PCF (DC-PCF) has been developed both for excitation and fluorescent signal collection but such a system requires a pre-chirp unit for nonlinear excitation.⁹ The ability to deliver the femtosecond light pulse in a hollow core over a broad range of wavelengths without the need for dispersion compensation and the simultaneous collection of signal through the solid silica cladding region gives the HC-PCF the advantage over other fibers used in single fiber nonlinear endomicroscopy. In this work, an endomicroscopy system formed by the integration of a single HC-PCF and a GRIN lens is used. The system is tuneable over a broad wavelength range of 750–850 nm without the need for the adjustment of dispersion compensation for each wavelength. The compactness of the system is improved by avoiding the use of the pre-chirp units, which also reduces the optical power loss of the system.

The schematic diagram of the experimental setup is shown in Fig. 1(a). It consists of a Ti: Sapphire laser (Spectra-Physics,

^{a)} Author to whom correspondence should be addressed. Electronic mail: mgu@swin.edu.au

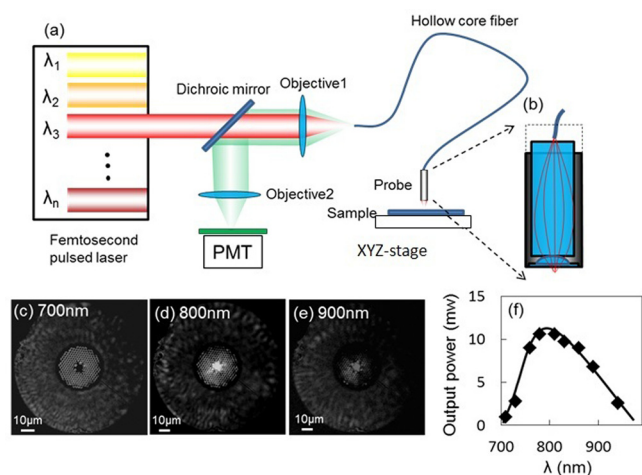


FIG. 1. (a) Schematic diagram of the experimental set-up for a broadband excitation and collection system for single fiber nonlinear endomicroscopy. PMT: photo-multiplier tube. (b) Enlarged part of the probe consisting of a HC-PCF and a GRIN lens. (c)–(e) Mode profiles of the HC-PCF for different wavelengths. (f) Output power at different wavelengths for the input power of 20 mW through a 1.5 m HC-PCF.

Mai Tai HP), which generates ultrafast optical pulses with pulse width 100 fs, repetition rate 80 MHz, and tuneable wavelengths around 690–1040 nm. Femtosecond pulses from the laser are coupled through a 40×0.85 NA objective to a HC-PCF (HC-800-01, NKT photonics, core diameter $9.5 \mu\text{m}$, core NA 0.2, cladding diameter $130 \mu\text{m}$) with a zero dispersion wavelength at 810 nm. For nonlinear imaging, a GRIN lens of numerical aperture 0.8 (GRINTECH, GT-MO-080-0415-810) is used in front of the output end of the fiber for focusing the laser beam to the sample on a scanning stage and simultaneously collecting the fluorescent signal back to fiber tip (Fig. 1(b)). The core and photonic crystal regions do not support the visible signal as it is out of the band gap of fiber. Thus, this part of the signal leaks out into the cladding region and propagates with total internal reflection at the air and solid silica interface of the solid silica cladding region after the outer acrylate coating of the fiber is removed. The fluorescent signal is finally focused to a photo-multiplier tube (PMT). Band pass filters (Schott—BG18 with transmittance $>50\%$ in the wavelength range 350–600 nm/Semrock—FF01-647/57-25 with pass band from 615–680 nm) are used before the PMT to filter the fluorescence signals from the reflected near infrared light.

Figures 1(c)–1(e) display the mode patterns in the HC-PCF at different wavelengths. Since wavelength 700 nm is out of the band gap of the photonic crystal in the HC-PCF, the light could not confine in the core, but distribute around the hole and the cladding region of the fiber (Fig. 1(c)). On the other hand, wavelength 800 nm is at the center of the photonic crystal band gap, the majority of light is confined inside the core of the HC-PCF (Fig. 1(d)), and the remaining light is leaked to the cladding area. However, wavelength 900 nm is close to the long wavelength edge of the photonic crystal band gap. Thus, the light confined in the core is decreased and the light leaked in the cladding increased (Fig. 1(e)) compared with the case in the wavelength of 800 nm (Fig. 1(d)). Figure 1(f) shows the fiber output power experimentally measured over the wavelength range for the given input power of 20 mW. Femtosecond pulses can be effectively

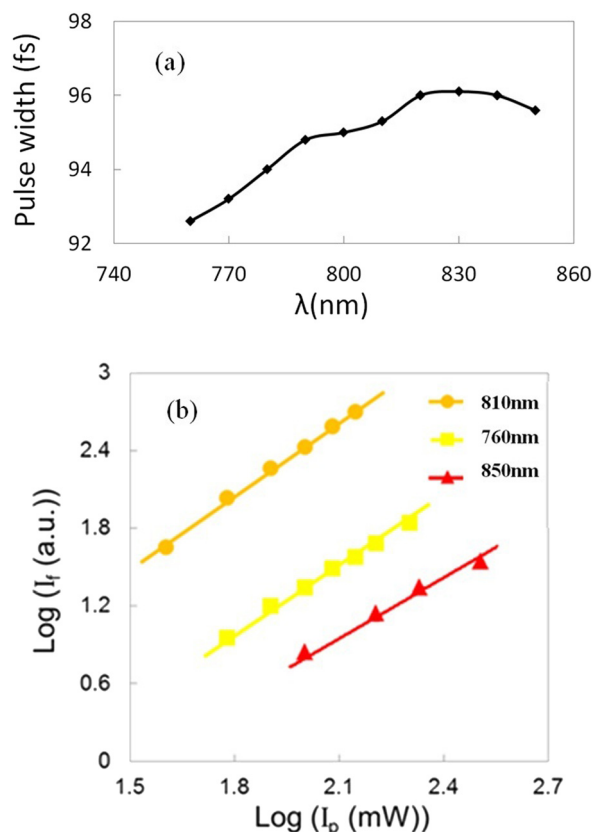


FIG. 2. (a) Pulse width measured at the output of the 1.5 m HC-PCF for different wavelengths at 100 mW. (b) Log-Log plot of the two-photon-excited fluorescence intensity (I_f) versus the excitation laser power (I_p) of fluorescent beads for wavelengths of 760 nm, 810 nm, and 850 nm.

delivered over a wavelength range of 750–850 nm through the core of the fiber.

Dry fluorescent microspheres of diameters $1 \mu\text{m}$ and $2 \mu\text{m}$ (Fluoresbrite[®] Yellow Green Microspheres, Polysciences Inc.) and rhodamine B (Sigma Aldrich) were used as test samples. The two-photon excitation peaks of the beads and rhodamine B dye are at ~ 805 nm and ~ 840 nm and their emission peaks are at ~ 485 nm and ~ 630 nm, respectively. The output pulse width measured at the output end of the 1.5 m HC-PCF at the 100 mW input power by a frequency-resolved optical gating (FROG) measurement setup (GRENOUILLE-008-50-USB, Swamp Optics) is less than 100 fs for the wavelength range from 750 nm to 850 nm as shown in Fig. 2(a). Therefore, the

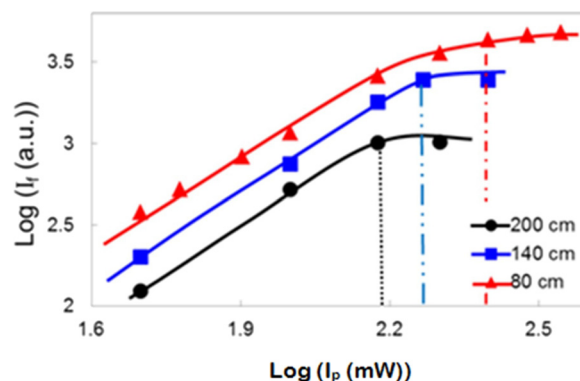


FIG. 3. Log-Log plot of the two-photon-excited fluorescence intensity versus the excitation laser power for different lengths of the fiber.

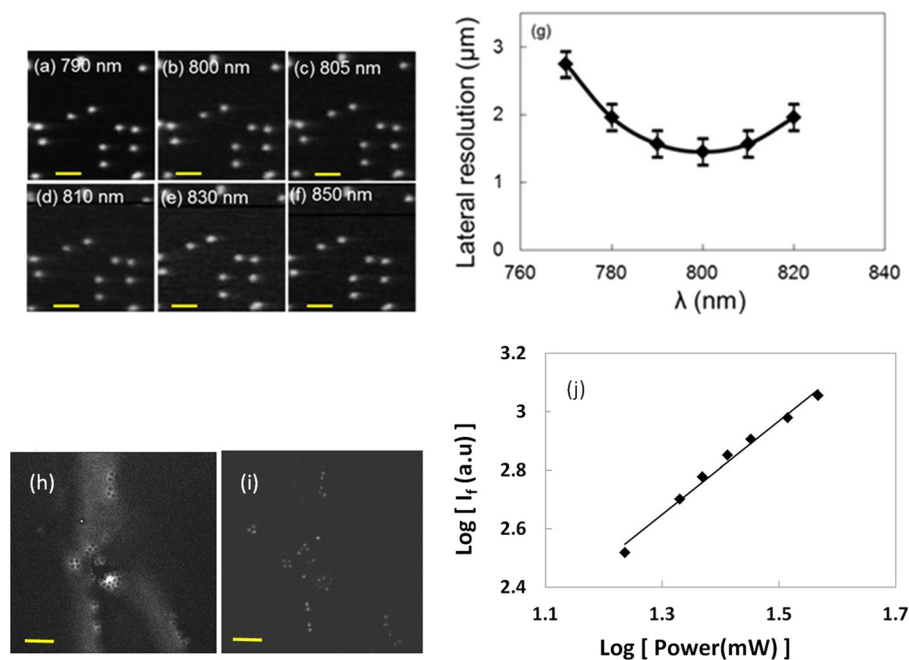


FIG. 4. (a)–(f) Two-photon fluorescence images of 1 μm fluorescent beads (scale bar: 5 μm). (g) Lateral resolution (full width at half maximum) of 1 μm fluorescent beads for the excitation laser power of 4.5 mW at the sample. (h)–(i) Two-photon fluorescence images of 2 μm fluorescent beads and the rhodamine B dye mixed sample (scale bar: 10 μm) at 800 nm; (h) with signal from rhodamine B dye only (signal from beads is blocked giving dark shadow spheres for them in the image), (i) with signal from fluorescent beads only (signal from rhodamine B dye is blocked). (j) Log-Log plot of two-photon-excited fluorescence intensity of rhodamine B dye versus excitation laser power at 800 nm.

compact nonlinear endoscope as shown in Fig. 1(a) can be used for different wavelengths without the requirement of dispersion compensation. Thus, different bio-markers can be efficiently used without the requirement for adjusting a pre-chirp unit. The dependence of fluorescence intensity detected by the PMT (Fig. 1(a)) on the excitation laser power at the sample for different wavelengths through the HC-PCF fiber was measured. A plot of the fluorescence intensity against the incident power on a logarithm scale for the central wavelengths 760 nm, 810 nm, and 850 nm fits a straight line with a slope close to 2 (Fig. 2(b)), indicating the fluorescence signal detected by the PMT is due to the two-photon excitation for the whole wavelength range.

Figure 3 shows the plot of the two-photon-excited fluorescence intensity versus the excitation laser power using dry fluorescent microspheres of diameter 1 μm as a sample. For this experiment, the two-photon-excited fluorescence intensity for the fiber with different lengths was measured by keeping the input coupling conditions same. The threshold power where the fiber nonlinearity starts to play a role is different for different lengths of the fiber, as shown in Fig. 3. The threshold power for fiber length of 200 cm, 140 cm, and 80 cm are 75 mW, 92 mW, and 125 mW, respectively. These threshold power levels are higher than the corresponding power levels that reported using other fibers,^{4,15} which is beneficial to high efficiency nonlinear endoscopy.

Figures 4(a)–4(f) show the two-photon-excited fluorescence images of the sample containing the 1 μm diameter dry fluorescent microspheres over the wavelength range, while Figs. 4(h) and 4(i) show the two-photon-excited fluorescence images at 800 nm of the sample formed by mixing the 2 μm diameter fluorescent beads and rhodamine B fluorescent dye solution in water and dried on the glass slide. In Fig. 4(h), fluorescence signal for imaging is collected only from rhodamine B dye (signal from beads is blocked giving dark shadow spheres for them in the image); while in Fig. 4(i), fluorescence signal from 2 μm beads only is collected for imaging (signal from rhodamine B dye is blocked). Fig. 4(g) shows

the lateral resolution (full-width at half maximum) for different wavelengths. The slight degrading in resolution at short wavelengths is due to the weak defocusing effect of the GRIN lens for the wavelength range. Fig. 4(j) shows the Log-Log plot of two-photon-excited fluorescence intensity of rhodamine B dye versus excitation laser power at 800 nm with a slope close to 2. It can be clearly seen that (a)–(f) confirms the simultaneous broadband excitation and collection ((h) and (i)), in the system shown Fig. 1(a), while (h)–(j) also demonstrate the multi-fluorophore two photon imaging ability of the system.

To summarize, broadband excitation and collection for a fiber-optic nonlinear endomicroscopy system has been realized by using a single piece of the HC-PCF integrated with a GRIN lens to operate in a NIR wavelength range from 750–850 nm. The dispersion compensation adjustment for different wavelengths is not required for nonlinear excitation over the range and thus multiple fluorescent markers with different excitation peaks can be used simultaneously. The broadband two-photon fluorescent signal can be collected through the cladding of the same piece of the HC-PCF. The optical power level for system operation is reduced by eliminating the requirement for lossy pre-chirp units for chromatic dispersion compensation. The HC-PCF has a higher nonlinear power threshold than other types of fibers previously used in fiber-optic nonlinear endoscopy. This endomicroscopy imaging system is easy to operate, versatile, compact, and possible to use low cost femtosecond pulsed fiber lasers.

The authors thank the Australian Research Council for its support.

¹W. R. Zipfel, R. M. Williams, and W. W. Webb, *Nat. Biotechnol.* **21**, 1369 (2003).

²B. R. Masters and P. T. C. So, *Opt. Express* **8**, 2 (2001).

³W. Denk and K. Svoboda, *Neuron* **18**, 351 (1997).

⁴D. Brid and M. Gu, *Appl. Opt.* **41**, 1852 (2002).

⁵D. Yelin, B. E. Bouma, S. H. Yun, and G. J. Tearney, *Opt. Lett.* **29**, 2408 (2004).

- ⁶L. Fu, X. Gan, and M. Gu, *Opt. Express* **13**, 5528 (2005).
- ⁷S.-P. Tai, M. C. Chan, T. H. Tsai, S.-H. Guol, L.-J. Chen, and C.-K. Sun, *Opt. Express* **12**, 6122 (2004).
- ⁸M. T. Myaing, D. J. MacDonald, and X. Li, *Opt. Lett.* **31**, 1076 (2006).
- ⁹L. Fu and M. Gu, *Opt. Lett.* **31**, 1471 (2006).
- ¹⁰L. Fu, A. Jain, H. Xie, C. Cranfield, and M. Gu, *Opt. Express* **14**, 1027 (2006).
- ¹¹H. Bao, J. Allen, R. Pattie, R. Vance, and M. Gu, *Opt. Lett.* **33**, 1333 (2008).
- ¹²H. Bao, S. Y. Ryu, B. H. Lee, W. Tao, and M. Gu, *Opt. Lett.* **35**, 995 (2010).
- ¹³W. Jung, S. Tang, D. T. McCormic, T. Xie, Y.-C. Ahn, J. Su, I. V. Tomov, T. B. Krasieva, B. J. Tromberg, and Z. Chen, *Opt. Lett.* **33**, 1324 (2008).
- ¹⁴D. R. Rivera, C. M. Brown, D. G. Ouzounov, I. Pavlova, D. Kobat, W. W. Webb, and C. Xu, *Proc. Natl. Acad. Sci. U.S.A.* **108**, 17598 (2011).
- ¹⁵H. Bao and M. Gu, *Opt. Lett.* **34**, 148 (2009).
- ¹⁶Y. Kremer, J.-F. Léger, R. Lapole, N. Honnorat, Y. Candela, S. Dieudonné, and L. Bourdieu, *Opt. Express* **16**, 10066 (2008).
- ¹⁷S. Kane and J. Squier, *Quantum Electron.* **31**, 2052 (1995).
- ¹⁸R. Du, R. Jiang, and L. Fu, *Opt. Express* **17**, 16415 (2009).
- ¹⁹D. Kim, H. Choi, S. Yazdanfar, and P. T. C. So, *Microsc. Res. Tech.* **71**, 887 (2008).
- ²⁰D. G. Ouzounov, K. D. Moll, M. A. Foster, W. R. Zipfel, W. W. Webb, and A. L. Gaeta, *Opt. Lett.* **27**(17), 1513 (2002).
- ²¹P. J. Mosley, W. C. Huang, M. G. Welch, B. J. Mangan, W. J. Wadsworth, and J. C. Knight, *Opt. Lett.* **35**, 3589 (2010).
- ²²F. Benabid, *Philos Trans. A* **364**, 3439 (2006).
- ²³J. C. Knight, F. Gérôme, and W. J. Wadsworth, *Opt. Quantum Electron.* **39**, 1047 (2007).
- ²⁴X. G. Xu, S. O. Konorov, J. W. Hepburn, and V. Milner, *Opt. Lett.* **33**, 1177 (2008).
- ²⁵D. H. Kim, J. U. Kang, and I. K. Ilev, *Electron. Lett.* **43**, 608 (2007).
- ²⁶W. Gobel, A. Nimmerjahn, and F. Helmchen, *Opt. Lett.* **29**, 1285 (2004).
- ²⁷C. L. Hoy, N. J. Durr, P. Y. Chen, W. Piyawattanametha, H. Ra, O. Solgaard, and A. Ben-Yakar, *Opt. Express* **16**, 9996 (2008).
- ²⁸Y. C. Wu, J. F. Xi, M. J. Cobb, and X. D. Li, *Opt. Lett.* **34**, 953 (2009).
- ²⁹R. L. Harzic, M. Weinigel, I. Riemann, K. König, and B. Messerschmidt, *Opt. Express* **16**, 20588 (2008).
- ³⁰C. J. Engelbrecht, R. S. Johnston, E. J. Seibel, and F. Helmchen, *Opt. Express* **16**, 5556 (2008).
- ³¹S. K. Vengalathunadakal, V. M. Murukesan, S. Padmanabhan, and P. Padmanabhan, *Opt. Eng.* **48**, 103601 (2009).